drag effects reinforce mass loss in that the amount of ablation increases with particle residence time (not velocity) in the shock layer. From Eq. (11) it can be seen that K_E is a dimensionless measure of the ratio of particle residence time in the shock layer to ablation time. For $K_E = 1/2$, $\bar{t} = t/(\Delta_s/U_\infty) = 1$, corresponds to the time required for complete ablation. This is deducible from Fig. 1 which shows that for zero drag ($K_D = 0$), no particles with values of $K_E \geqq 1/2$ survive; this value can be used to determine the largest size particle that will not survive. That is [see Eq. (8)] particles satisfying the condition

$$r_e \leqq (k_m Nu_m \Delta T_m \Delta_s/\sigma Q^* U_\infty)^{1/2}$$

would be predicted not to survive the shock environment. The reinforcing effects are expected to be a strong function of r_e since K_D varies as r_e^{-1} and K_E as r_e^{-2}. For very low velocities and small particle radii the analysis becomes invalid due to the fact that the gas velocity has been assumed negligible relative to the particle velocity and the assumption of constant drag coefficient break down. Nevertheless, this should cause the predictions to be conservative since the drag coefficient increases as particle Reynolds number goes to zero. As was pointed out the model used is idealized in that diffusion and phase change kinetics have been ignored; thus the results are representative of a bounding case. A more detailed treatment is given in Ref. 5.

References

[1] Waldman, G. D. and Reinecke, W. G., "Particle Trajectories, Heating and Breakup in Hypersonic Shock Layers," *AIAA Journal*, Vol. 9, No. 6, June 1971, pp. 1040–1048.

[2] Hoglund, R. F., "Recent Advances In Gas-Particle Nozzle Flows," *ARS Journal*, Vol. 32, 1962, pp. 662–671.

[3] Gilbert, M., Allport, J., and Dunlap, R., "Dynamics of Two-Phase Flow in Rocket Nozzles," *ARS Journal*, Vol. 32, 1962, pp. 1929–1930.

[4] Carlson, D. J. and Hoglund, R. F., "Particle Drag and Heat Transfer in Rocket Nozzles," *AIAA Journal*, Vol. 2, No. 11, Nov. 1963, pp. 1980–1984.

[5] Jaffe, N. A., "Particle Deceleration and Heating In a Hypersonic Shock Layer," TN-73-18, Feb. 1973, Aerotherm, Mountain View, Calif.

Inviscid Swirling Flows through a Choked Nozzle

C. T. HSU* AND A. D. DEJOODE†

Iowa State University, Ames, Iowa

FOR a steady, inviscid, isoenergetic and homentropic, swirling flow through a circular, constant-area pipe, the radial distribution of axial Mach number was obtained[1,2] previously in closed form solutions as follows:

$$M_a^2 = C_1/\{1-(\alpha^2 R^2)/r^2 - [(\gamma-1)/2]C_1\} \quad (1)$$

for a free-vortex flow in which the tangential velocity decreases inversely with radial distance, and

$$\frac{[1+(\gamma-1)M_a^2/2]}{[1+(\gamma-1)M_a^2/4]} = C_2[1-(\gamma-1)\omega^2 r^2/2a_o^2] \quad (2)$$

for a forced-vortex flow in which the tangential velocity increases linearly with radial distance, where

$$\alpha(r) = [(\gamma-1)/2]^{1/2}\Gamma/a_o R \quad (3)$$

is the swirling parameter. C_1 and C_2 are two arbitrary constants to be determined; r denotes the radial distance; R, the radius of the pipe; γ, the ratio of specific heats; ω, the angular velocity of solid body rotation; a_o, the stagnation sound speed; and $\Gamma = vr$, the circulation per unit radian evaluated at various radial distances.

In a real nozzle flow, a Rankine-combined vortex, i.e., a forced vortex core of radius r_c with outer free-vortex flow is more likely[3] to occur. In this case, superposition of these two types of vortex flows can be directly obtained from Eqs. (1) and (2). Then, the mass flow rate can also be superimposed for a given stagnation pressure p_o, a stagnation temperature T_o, and the pipe area, as follows:

$$\dot{m}(\alpha_c, r_c, C_1, C_2) = \dot{m}_1(\alpha_c, r_c, C_1) + \dot{m}_2(\alpha_c, r_c, C_2) \quad (4)$$

where

$$\dot{m}_1 = 2\pi p_o\left(\frac{\gamma C_1}{R' T_o}\right)^{1/2}\int_{r_c}^{R}\left[1-\frac{\alpha_c^2 R^2}{r^2}-\frac{\gamma-1}{2}C_1\right]^{1/(\gamma-1)} r\,dr \quad (4a)$$

represents the portion of free vortex flow, R' is the gas constant, and where

$$\dot{m}_2 = 4\pi p_o[\gamma/(\gamma-1)R' T_o]^{1/2} C_2^{(\gamma+1)/(2-2\gamma)}\int_0^{r_c}\left[2-C_2\times\left(1-\frac{\alpha_c^2 r^2 R^2}{r_c^4}\right)\right]^{1/(\gamma-1)}\left[C_2\left(1-\frac{\alpha_c^2 r^2 R^2}{r_c^4}\right)-1\right]^{1/2} r\,dr \quad (4b)$$

represents the portion of forced vortex core flow, where

$$\alpha_c = \left(\frac{\gamma-1}{2}\right)^{1/2}\frac{\omega r_c^2}{a_o R} = \left[\frac{\text{max. swirl energy}}{\text{total energy}}\right]^{1/2}\frac{r_c}{R} \quad (5)$$

is now the maximum swirling parameter evaluated at r_c. Also, at r_c, M_a is continuous, so C_1 is related to C_2 from Eqs. (1) and (2) by

$$C_1 = 4\left[C_2\left(1-\frac{\alpha_c^2 R^2}{r_c^2}\right)-1\right]/(\gamma-1)C_2 \quad (6)$$

When $\dot{m}$ is choked at the pipe or delivers the maximum mass flow rate for a given α_c and r_c, the complete flow nature in the pipe can be determined by obtaining C_1 or C_2 from the choking condition,

$$\partial\dot{m}/\partial C_1 = 0 \quad \text{or} \quad \partial\dot{m}/\partial C_2 = 0 \quad (7)$$

The following examples were evaluated by numerical computations for C_1 or C_2 from Eq. (7), i.e., to find a range of C_1

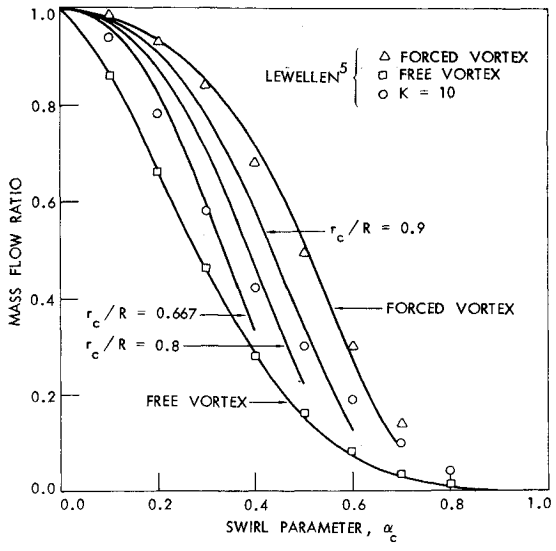

Fig. 1 Choked mass flow ratio vs swirl parameter.

Received February 28, 1973; revision received May 25, 1973. This research was supported by the Engineering Research Institute, Iowa State University.

Index category: Nozzle and Channel Flow.

* Professor, Department of Aerospace Engineering, and Engineering Research Institute. Member AIAA.

† Formerly graduate student, Department of Aerospace Engineering; now with Rockwell International, Columbus, Ohio. Associate Member AIAA.

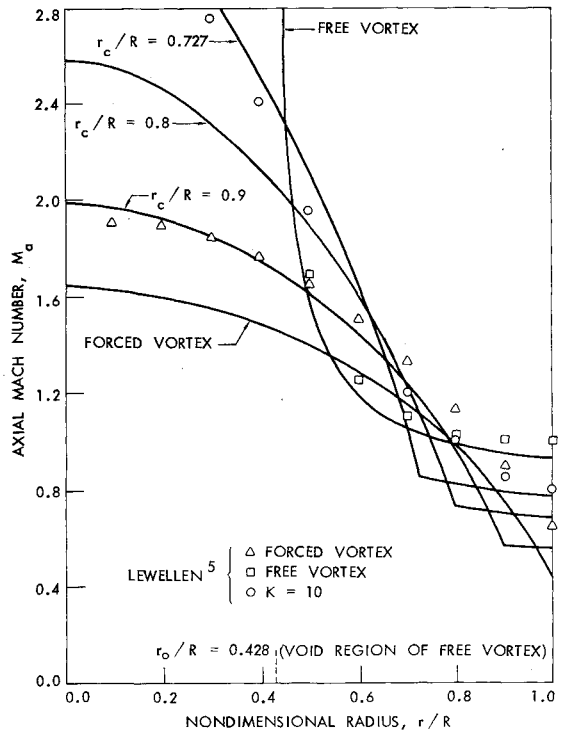

Fig. 2 Radial distribution of axial Mach number in a choked nozzle throat for $\alpha_c = 0.4$.

that would change the sign of $\partial\dot{m}/\partial C_1$ in Eq. (7). With proper computer programing, this only requires 2–3 sec of computation time in an IBM 360-65. Thus, the present analysis avoids the numerical solutions of two simultaneous differential equations[5] for this problem.

It should be mentioned than an analytical expression for Eqs. (4a, 4b, and 7) were also obtained by closed form integrations.[4] These expressions are too lengthy to include here. The results

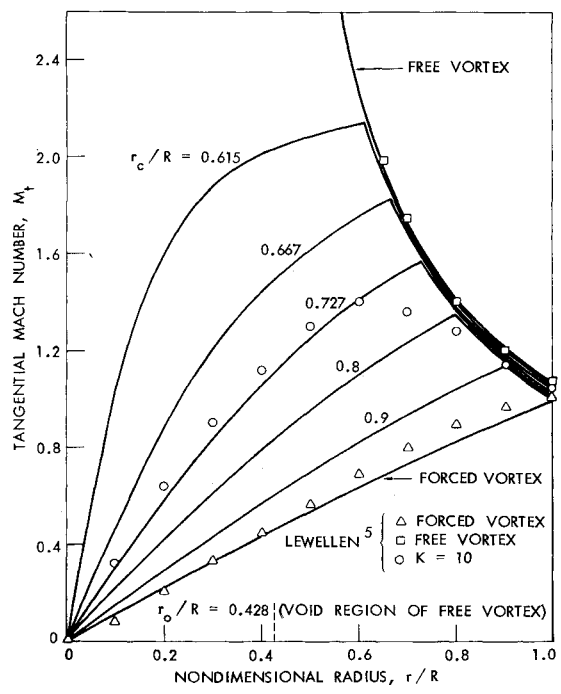

Fig. 3 Radial distribution of a tangential Mach number in a choked nozzle throat for $\alpha_c = 0.4$.

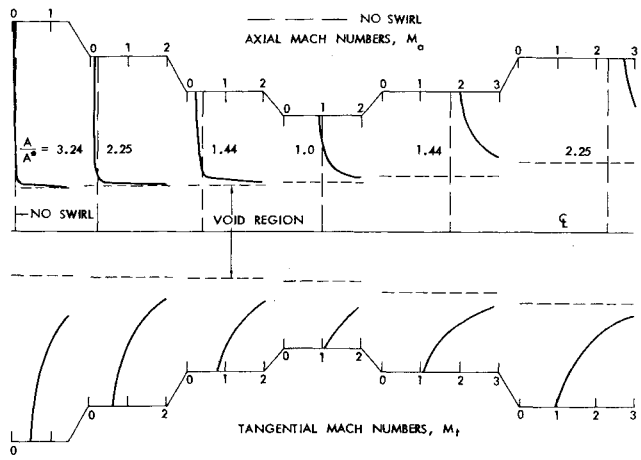

Fig. 4 Approximate axial and tangential Mach number distribution in a convergent-divergent nozzle, $\alpha_c = 0.4$.

were consistent with that of the above numerical integration to three decimal places for $\alpha_c \leqq 0.4$ in the forced vortex case. However, the present computer programing does not work for higher values of α_c in the forced vortex case as well as the entire range of α_c for the free vortex case. Further investigation of this problem will be reported later.

Figure 1 shows the mass flow ratio vs α_c with various core radii r_c. This mass flow ratio refers to the choked swirling mass flow divided by the corresponding conventional one-dimensional value. Note that α_c has a limiting value for a given r_c as indicated in Eq. (5). Figures 2 and 3 represent, respectively, the radial distribution of the axial and tangential[1] Mach number for $\alpha_c = 0.4$. The present work should give results identical to Lewellen et al.[5] if the same swirling function $\alpha(r)$ is used. Deviations shown in the aforementioned figures are due to the slightly different swirling function used in each case. In the present case, a Rankine-combined vortex flow of exact, solid body rotation core and outer potential vortex flow was assumed. In Lewellen's case, the following swirling function is assumed:

$$\frac{\alpha(r')}{\alpha_c} = \frac{1-\exp[-K\Psi^*(r')]}{1-\exp[-K\Psi^*(1)]} \tag{8}$$

where $r' = r/R$, $\Psi^*(r')$ is a normalized stream function for choked condition and K is a parameter that plays the role of Reynolds number. This swirling function exhibits a vortex flow of approximate solid body rotation in the core and approximate potential vortex flow in the outer portion. This is because, in Lewellen's case, for small values of K, $\alpha(r')$ which may be expanded into a power series of K, is approximately proportional to the mass flow ratio

$$\alpha(r')/\alpha_c \doteq \Psi^*(r')/\Psi^*(1) \tag{9}$$

instead of the nozzle area ratio for the present case as shown in Eq. (3). Also, for large values of K, $\alpha(r') \doteq \alpha_c$. This swirling function exhibits a smoother Mach number distribution for moderate value of K. Note that the case of $K = 10$ roughly corresponds to $r_c/R = 0.7273$ in the present case.

Assuming a free vortex flow remains as a free vortex flow in a slowly varying convergent-divergent nozzle, the present solutions may be extended to any fictitious constant-area nozzle section of sufficient length where the radial velocity together with its axial derivatives can be neglected.[2] For a given choked mass flow, C_1 can be evaluated from Eq. (4a) and M_a from Eq. (1). The axial variation of Mach numbers is shown in Fig. 4 for different nozzle section areas: $A/A^* = 3.24$, 2.25, and 1.44. Two values of C_1 are always obtained from Eq. (4a). One corresponds to a subsonic flow in the convergent portion and the other to a supersonic flow in the divergent portion. The axial Mach numbers are usually smaller than the corresponding value of one-dimensional nozzle in the convergent portion, but they are larger

in the divergent portion. This is probably because the void region gradually grows as the axial Mach number is increased. The radii of void regions near the nozzle axis were obtained by setting the denominator of Eq. (1) equal to zero.

References

[1] Hsu, C. T., "Swirling Nozzle Flow Equations from Crocco's Relation," *AIAA Journal*, Vol. 9, No. 9, Sept. 1971, pp. 1866–1868.

[2] Hsu, C. T., "Errata: 'Swirling Nozzle Flow Equations from Crocco's Relation,'" *AIAA Journal*, Vol. 10, No. 3, March 1972, p. 368.

[3] Batson, J. L. and Sforzini, R. H., "Swirling Flow through a Nozzle," *Journal of Spacecraft and Rockets*, Vol. 7, No. 2, Feb. 1970, pp. 159–163.

[4] DeJoode, A. D., "Mach Number Distribution and Mass Flow Rate for Swirling Flow in a Choked Nozzle Throat," MS thesis, Feb. 1973, Iowa State Univ., Ames, Iowa.

[5] Lewellen, W. S., Burns, W. J., and Strickland, H. J., "Transonic Swirling Flow," *AIAA Journal*, Vol. 7, No. 7, July 1969, pp. 1290–1297.

A Finite Element Method for the Optimal Design of Variable Thickness Sheets

M. P. Rossow* and J. E. Taylor†

The University of Michigan, Ann Arbor, Mich.

Introduction

THE nature of recent research work in the field of structures optimization is summarized (exclusive of Russian and East European activity) by Niordson and Pedersen in Ref. 1. There is evidence from their survey as well as from other sources of a trend toward greater emphasis on topics related to numerical solution. Our development of a finite element interpretation for the prediction of optimal design follows this trend. We particularly seek to establish useful means for handling two-dimensional design problems.

Several recent papers on general methods for the numerical solution of design problems relate to our work. To name a few, Haug et al.[2] developed a steepest descent procedure to calculate the optimal design of piecewise uniform structures. Also Maier et al.[3] demonstrated how the problem of designing for maximum safety relative to collapse of plane stress structures can be formulated as a linear programing problem, through the use of finite element modeling of the structure. Dafalias and Dupuis[4] made use of a discretization scheme to obtain their procedure for the solution of optimum beam design problems. Aspects of numerical solution in flutter optimization problems were discussed by Ashley and McIntosh.[5]

In some early automated design programs, a design prediction was obtained by iteration on the computer between independent design and analysis elements of a program. In contrast, our formulation amounts to having the finite element discretization incorporated into a direct design procedure. This formulation is demonstrated, and the character of the governing equations for the discretized structure is established. An example application of the formulation is provided.

Received March 26, 1973; revision received June 18, 1973. Support was received from the National Science Foundation for the research reported in this Note.

Index category: Structural Design, Optimal.

* Postdoctoral Fellow, Department of Applied Mechanics and Engineering Science.

† Associate Professor, Departments of Aerospace Engineering, and Applied Mechanics and Engineering Science. Member AIAA.

Many of the considerations associated with the problem formulation reported in this Note are treated in greater detail in the thesis of Rossow.[6]

Problem Formulation

The optimality criterion to be used in this Note is that of maximum stiffness for a given volume of material. More precisely, if $W[t]$ represents the loss in potential of the edge loads applied to the sheet of variable thickness t, then an optimal design t^* is defined by the relation

$$W[t^*] = \min_t W[t] \tag{1}$$

All admissible designs t are required to satisfy the volume constraint

$$\int_A \int t\, dA = V_o \tag{2}$$

Here A is the region in the x-y plane occupied by the sheet, and V_o is the specified volume of material.

It is convenient for subsequent developments to replace the quantity $W[t]$ by the potential energy of the sheet, $P[t]$. By Clapeyron's Theorem, we have

$$P[t] = -W[t]/2 \tag{3}$$

Thus, the maximum stiffness design problem can be restated as the problem of finding t^* such that

$$P[t^*] = \max_t P[t] \tag{4}$$

where t satisfies Eq. (2).

The potential energy for an elastic sheet in a state of plane stress is

$$P[t] = \frac{1}{2}\int_A \int \boldsymbol{\varepsilon}^T \mathbf{c}\boldsymbol{\varepsilon} t\, dA - \int_S (Xu + Yv)\, dS \tag{5}$$

where $u = u(x, y)$ and $v = v(x, y)$ are the displacements of the sheet in the x and y coordinate directions, and $t = t(x, y)$ is the sheet thickness. The elastic strain $\boldsymbol{\varepsilon}$ in Eq. (5) is given by

$$\boldsymbol{\varepsilon}^T \equiv \{\partial u/\partial x, \partial v/\partial y, \partial u/\partial y, \partial v/\partial x\} \tag{6}$$

while the elastic constants $\mathbf{c}$ represent

$$c = \frac{E}{1-\nu^2}\begin{bmatrix} 1 & \nu & 0 \\ \nu & 1 & 0 \\ 0 & 0 & (1-\nu)/2 \end{bmatrix} \tag{7}$$

Here E symbolizes Young's modulus and ν the Poisson ratio. S designates that portion of the boundary of A where the components X and Y of the traction vector are specified.

Equation (4) together with Eq. (2) defines an isoperimetric problem in the calculus of variations (cf. Ref. 6). Its solution must satisfy the Euler equations with respect to t of the functional comprised of the potential energy augmented by the volume constraint. The two equilibrium equations associated with u and v must, of course, be satisfied at the same time. (These equations are sufficient for optimality as well as necessary; see, for example, Ref. 8.)

Finding the solution of this system of three simultaneous partial differential equations will, in general, require the use of numerical methods. A particular approximating scheme based on a finite element representation of the potential energy of the sheet will now be presented.

Let the region A occupied by the sheet be divided into a mesh of n elements and approximate the thickness function t in element i, $i = 1, 2, \ldots, n$, by a uniform value τ_i. After also approximating the displacement field within element i in the usual finite element manner, the first term on the right-hand side of Eq. (5) when evaluated over element i yields

$$\frac{\tau_i}{2}\sum_{r=1}^{p}\sum_{s=1}^{p} K_{rs}{}^i \delta_r{}^i \delta_s{}^i \equiv \tau_i U_i(\delta) \tag{8}$$

Here $\delta_r{}^i$ denotes a local nodal displacement, $K_{rs}{}^i$ is a member of the element stiffness matrix, and p is the number of displace-